Journal of Geospatial Surveying (2023) 3:1
DOI: http://doi.org/10.4038/jgs.v3i1.47

ORIGINAL ARTICLE

Assessment of Ecological Disturbance on Indian Sundarbans with Special Reference to Amphan Cyclone by Using Geospatial Technology

Prakash, S., Varghese, A.*, Amrutha, A. S., Baiju, K. R.

Dr. R. Satheesh Centre for RS & GIS, School of Environmental Sciences, Mahatma Gandhi University, Kottayam, Kerala, India

ARTICLE INFO

Article history:
Received 31 January 2023
Received in revised form 25 March 2023
Accepted 4 April 2023
Available online 18 April 2023

Keywords:
Sundarbans
Cyclone
NDVI
EVI
Salinity
LST

ABSTRACT

The mangrove ecosystem of Sundarbans region plays a significant ecological and socio-economic role in both India and Bangladesh. An increase in coastal human settlements makes the area more vulnerable to natural disasters such as tsunamis and cyclones. Mangroves, as an exclusive group of plants, provide many ecological services such as reducing the impacts of cyclonic storms and gales and minimizing the sea level rise due to global warming. Sundarbans were facing immense destruction due to super cyclones during the past years. The present study investigated the ecological disturbance caused by the cyclone Amphan in Indian Sundarbans using remote sensing multispectral imagery. The pre and post-cyclonic Landsat data were analyzed to quantify the damaged area in Sundarbans due to the effect of the cyclone, Amphan. Normalized Vegetation Index (NDVI) and Enhanced Vegetation Index (EVI) were used to estimate the vegetative changes or losses that occurred due to the cyclone. Normalized Difference Water Index (NDWI), Normalized Difference Bareness Index (NDBaI) and Normalized Difference Salinity Index (NDSI)) were the other indices used to study the effects of cyclone. The study found that from pre to post-cyclonic period, mangroves reduced from 1,851.88 km^2 to 1,643.74 km^2 and about 50.18 km^2 of vegetation becomes sparse. High salinity values were observed during the post-cyclonic period which indicated that the super cyclone resulted in saltwater intrusion. From pre to post cyclone, NDBaI results showed an increase in barren land from 908.13 km^2 to 1,365.57 km^2.

1 Introduction

The mangroves are a group of plants with remarkable ecological importance that mainly inhabit areas that are washed by the tides. Extensive and deep-rooted system of mangroves helps in protecting coastline from erosion, assist in reclaiming land and purify water through their ability to absorb pollutants, including heavy metals. Mangrove forests are disappearing at an alarming rate in many parts of the world as a result of ongoing natural and anthropogenic activities. Sundarbans is the largest single patch of mangrove forest in the world, stretching over the southern coast of Bangladesh and India, offering coastal protection to millions of people. However, storm protection provided by this unique mangrove ecosystem has not yet been quantified in terms of its economic value (Akber et al., 2018). A scientific study reports that mangrove forests in the Sundarbans reduced both wind and storm surge intensity during cyclone Sidr (Paul, 2009; Sakib, 2015). A rapid rise in sea surface temperature induced by climate change makes the east coast of India extremely vulnerable to tropical cyclones (Mishra and Vanganuru, 2020). According to climate models and observations, tropical cyclone intensity is expected to increase under future climate scenarios, making coastal communities more vulnerable to these natural disasters. However, it is not possible to stop disasters, but their impacts can be minimised using a range of management approaches, (response, recovery, prevention/reduction and preparedness).

Remote sensing and GIS are efficient and accurate tools to provide useful information in every phase of cyclone disaster management (Hoque et al., 2017). An important contribution of satellite remote sensing is the use of repeated high spatial resolution satellite images before and after an event, such as a cyclone, to assess impacts and monitor recovery progress (Klemas, 2009; Krishnamohan et al., 2014). In addition, satellite remote sensing can be used to track tropical cyclones and predict landfall

* Corresponding author: A. Varghese, Dr. R. Satheesh Centre for RS & GIS, School of Environmental Sciences, Mahatma Gandhi University, Kottayam, Kerala, India.

E-mail address: abin.udumbanattu@gmail.com (A. Varghese).

accurately. The study presented here focuses on the assessment of ecological disturbance caused by cyclone Amphan in Indian Sundarbans using Geospatial tools. This study is expected to contribute to the realisation of the storm protection function of the Sundarbans mangrove forest and, in turn, influence the conservation policies of the region. Spectral indices are a good approach to distinguish land cover types (Rasul et al., 2018). Dutta et al., (2015) conducted similar study on ecological disturbance caused by cyclones of different intensities (eg: SIDR, Rashmi and Aila) striking the mangrove at different phonological stages using MODIS Global Disturbance Index (MGDI) based approach. Simple vegetation indices (Vis) including Normalized Difference Vegetation Index (NDVI), Enhanced Vegetation Index (EVI), Leaf Area Index (LAI), can highlight plant intrinsic properties that are closely related to leaf greenness and vigour (Baloloy et al., 2020; Rouse et al., 1973). Moisture, vegetation cover, bare areas and soil condition are essential to analyse the vegetation health of an ecosystem (Dutta et al., 2020). The present study analyses different indices such as NDVI, EVI, Normalised Difference Water Index (NDWI), Normalised Difference Salinity Index (NDSI) and Normalized Difference Bareness Index (NDBaI) of pre and post cyclonic periods to analyse the changes that occurred after the super cyclone. NDVI and EVI are some of the most widely used techniques to monitor the vegetation (Jaman et al., 2019). Moreira et al., (2015) identified the saline-exposed soils, using several indices of salinity such as Salinity Index (SI), Normalized Difference Salinity Index (NDSI), and correlated with electrical conductivity values. Statistical correlations between electrical conductivity (EC) and remote sensing spectral indices indicated that the SI correlated most strongly with EC (Elhag and Bahrawi, 2017).

2 Materials and Methods

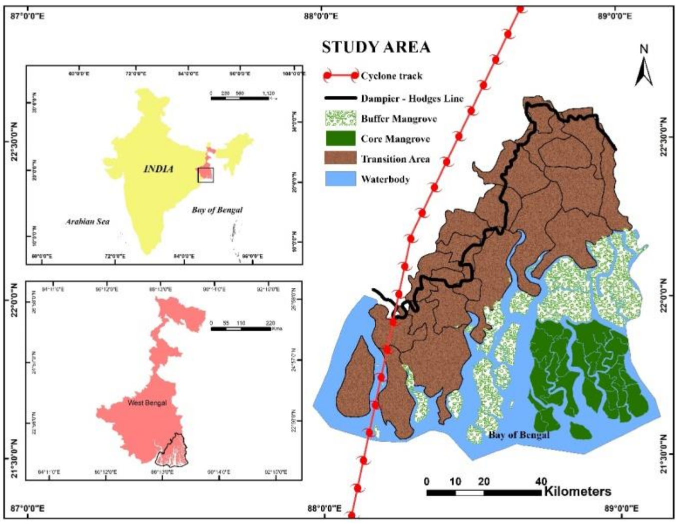

Fig. 1: Study area.

The study was carried out in the Indian part of Sundarbans which lies between 21° 36′ N 88° 0′ E – 22° 38′ N 89° 0′ E, which is the world's largest contiguous mangrove forest (Fig. 1). Boundaries of Indian Sundarbans Delta (ISD) is defined by boundaries Ichamati-Raimangal River in the east, the Hoogli River in the west, the Gulf of Bengal in the south, and the Dampier and Hodges line drawn in 1829–1830 in the north. The region is susceptible to cyclonic activity and has a prolonged history of cyclones hitting the area, resulting in the loss of lives and properties.

2.1 Land Use Land Cover Mapping

Landsat 8 OLI/TIRS images of year 2020 and 2021 were used for the entire study. Cloud free images of January 2020 (pre cyclone) and April 2021 (post cyclone) were downloaded from USGS Earth Explorer. All images were geometrically corrected for pre-processing. Using the maximum likelihood classification method, supervised classification was employed to generate Land Use Land Cover (LULC) maps for the pre- and post-cyclonic periods of the years 2020 and 2021. Over the last two decades, supervised maximum likelihood classification techniques have been used worldwide to study mangrove LULC (Akbar Hossain et al., 2022). Based on literature reviews and high resolution imagery from Google Earth as reference data, 6 LULC categories as healthy mangroves, unhealthy mangroves, water-bodies, aquaculture, agriculture and plantation with built up areas were identified in the study area. Random sampling method was adopted for accuracy assessment (Akbar Hossain et al., 2022).

2.2 Calculation of NDVI, EVI, NDWI, NDSI, NDBaI

Using the radiance rescaling factors provided in the metadata file of satellite images, all bands were converted to top of the atmosphere (TOA) spectral radiance and the atmospheric corrected images were used for the calculation of different indices using the equations in Table 1. Zonal statistics was performed for each index with LULC to evaluate vegetation health of different LULC classes.

Table 1: Formulae used for the calculation of indices.

Index Name	Formula
Normalised Difference Vegetation Index (NDVI)	(NIR-RED)/(NIR+RED)
Enhanced Vegetation Index (EVI)	2.5 x ((NIR-RED)/(NIR+6 × RED -7.5 ×BLUE+1))
Normalised Difference Water Index (NDWI)	(GREEN-NIR)/(GREEN+NIR)
Normalised Difference Salinity Index (NDSI)	(GREEN-SWIR)/(GREEN+SWIR)
Normalized Difference Bareness Index (NDBaI)	(NIR – TIR)/(NIR+TIR)

3 Results and Discussion

3.1 Patterns of LULC Changes

Six LULC classes were identified in the study area with an overall accuracy of 85.3% (Ghosh et al., 2015). Fig. 2 shows the representation of the total area of LULC during the temporal period of analysis.

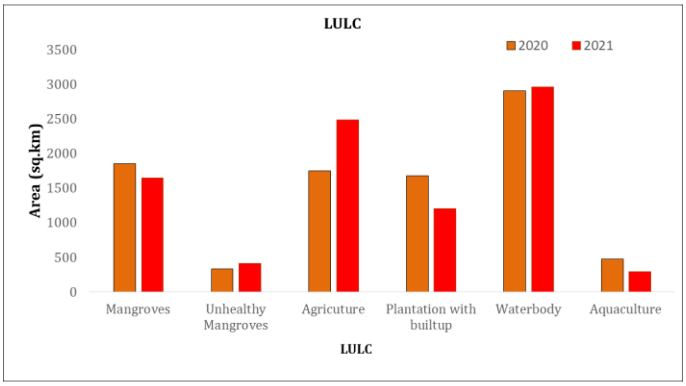

Fig. 2: Total area of each LULC class during pre and post cyclone period.

LULC analysis shows that majority of the vegetated area had drastically changed after the cyclonic period. Mangrove area coverage decreased from 1,851.88 km² to 1,643.74 km² and unhealthy mangroves increased from 332.48 km² to 412.63 km², indicating that Amphan has caused damage and fragmentation to the mangrove vegetation. On the other hand aquaculture decreased from 5.27% to 3.25% while water-bodies increased from 32.34% to 32.91% indicating a loss of aquaculture areas due to flooding (Ghosh et al., 2015). Agriculture area increased from 19.43% of the total area in 2020 to 27.61% in 2021 (an increase of 42.10%), indicating a shift in the LULC dynamics. Open forests are being converted to agriculture in order to maximise yield, and are destroyed uncontrollably to accommodate the surging population, resulting in a decrease in mangrove habitats (Dutta et al., 2015). 28% change in plantations with the built up class occurred from pre-cyclonic to post-cyclonic periods, indicating that not only vegetative losses occurred, but human resources were also damaged due to Amphan. Most of the forest degradation occurred in the western part of the Indian side, near populated areas and along the path of the cyclone, including where it made landfall (Mishra et al., 2021).

3.2 NDVI Patterns in the Study Area

From Table 2, it can be seen that the mean NDVI values for most of the LULC categories have decreased after the cyclone. For mangrove forests, the average NDVI values have declined from 0.3042 in 2020 to 0.043 in 2021 (Table 2), which indicates a decline in the healthy forest covers and an increase in open patches/non-vegetated cover (Kamble et al., 2013; Mishra et al., 2021; Mondal et al., 2021). Some studies may conclude unsustainable and illegal harvesting of forest resources as the major contributory factor to spatial and temporal changes in the tree cover of Sundarbans. The temporal NDVI maps of the study for pre and post cyclonic period are shown in Fig. 3. Plantations mapped in the study area exist mostly as homestead orchards. Plantation with built up areas shows an increase in NDVI values from 0.1378 to 0.309.

Table 2: Index values for each LULC class during pre and post cyclonic periods.

LULC	Indices					
	NDVI		EVI		NDSI	
	2020	2021	2020	2021	2020	2021
Water-bodiies	-0.40	-0.511	-0.492	-0.610	0.945	0.964
Agriculture	0.003	-0.014	0.007	-0.013	0.692	0.711
Mangroves	0.30	0.043	0.509	0.068	0.804	0.762
Plantations with built up area	0.13	0.309	0.218	0.518	0.742	0.810
Aquaculture	-0.22	-0.309	-0.294	-0.395	0.862	0.911
Unhealthy Mangroves	0.177	0.136	0.282	0.216	0.790	0.799
Agriculture	0.003	-0.014	0.007	-0.013	0.692	0.711

3.3 EVI Patterns in the Study Area

Fig. 3 shows the EVI for pre and post-cyclone which indicates the richness of vegetation. EVI values declined after cyclonic events, indicating that almost every part of the Sundarban mangrove forest was degraded and fragmented during the cyclone Amphan. A rapid change in EVI from 0.5099 to 0.0682 was observed in areas with mangroves and an increase in plantation with built up areas from 0.2186 to 0.5189. The EVI results also show that the cyclone had a significant impact on agricultural areas in the region because this cover is more sensitive than mangrove vegetation, which has roots that are more deeply embedded in the soil. There has been an alarming increase in the rate of change in parts of the western, eastern, and central Sundarbans. Mishra et al., (2021) discovered that the change in the landscape caused by Amphan was comparably greater in the Indian Sundarbans area (87%) than in Bangladesh (83%).

3.4 Normalised Difference Salinity Index

Stressed vegetation could be an indirect sign of the presence of salt in the soils. NDSI values indicate that salinity increased elsewhere from pre to post cyclone, except in the mangrove class. The increase in NDSI value indicated that the cyclone had resulted in a high level of salt water intrusion even in faraway places from the coastal line. Sundarban mangroves are extremely resistant to extreme weather conditions (Giri et al., 2007) and only a slight difference was observed in NDSI values of the mangrove class after the cyclonic period.

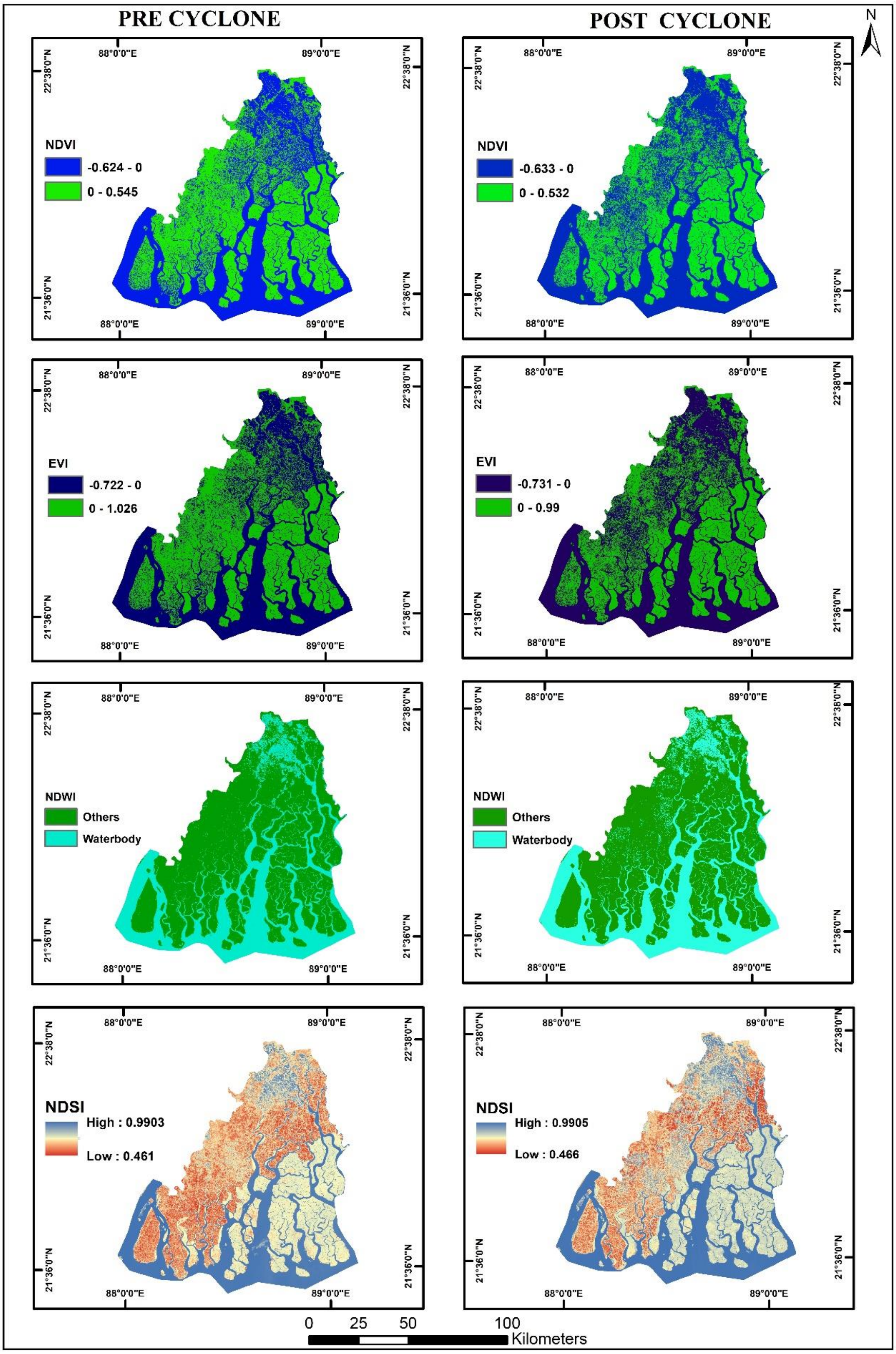

Fig. 3: Map of indices (NDVI, EVI, NDWI, and NSDI from top to bottom) for the pre (left) and post (right) cyclonic period.

The highest NDSI values were observed in water-bodies for both pre and post cyclonic periods. Higher salinity values indicate greater water stress and less water content (Hunt Jr and Rock, 1989). LULC pattern study showed a gradual decrease in the area of aquaculture, as an increase in salinity triggers the death of juvenile fishes, resulting in a decline in this class.

Table 3: Summary of the LULC classification using NDBaI and NDWI during the pre and post cyclone period.

Indices	Category	2020		2021		2020 - 2021	
		Area (km²)	Area (%)	Area(km²)	Area (%)	Area change	% change
NDWI	Water-bodies	3084.268	34.29	3211.844	35.71	160.576	-5.20
NDBaI	Water-bodies	5733.49	63.74	5937.56	66.01	-204.07	-3.53
	Vegetation	2352.97	26.15	1691.44	18.80	-661.52	-28.11
	Barren land	908.13	10.09	1365.57	15.18	457.44	50.37

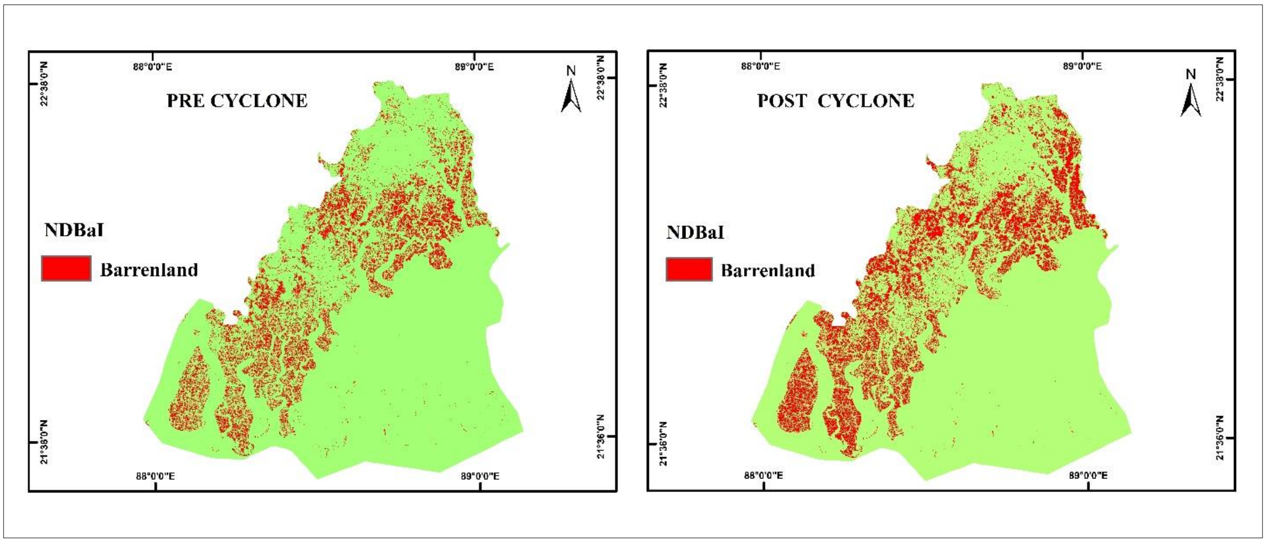

Fig. 4: Map of NDBaI during the pre and post cyclonic period.

3.5 Normalised Difference Water Index

The results of the index can range from -1 to +1. Positive values are assigned to water features, whereas zero or negative values are assigned to soil and terrestrial vegetation features (McFeeters, 1996). Values greater than 0.3 were considered as water-bodies, while negative values were considered as vegetation, and values between 0 and 0.2 were considered as buildup areas. Water-bodies was delineated using these values and about 34.29% of the total area (3,084.268 km²) was considered as water-bodies in 2020. Table 3 shows that the area of water-bodies increased by 5.20% with an area change of 160.576 km².

3.6 Normalised Difference Bareness Index

NDBaI values ranged from -1 to +1. Values greater than 0 were demarcated as barren land, -0.25 to 0 as vegetation and < -0.25 as water-bodies (Chen et al., 2006). Table 3 shows that the total bare land area obtained from the index before Amphan was 908.13 km², which is about 10.09% of the total area. A significant increase, of about 50.37%, was observed in barren land after the cyclone. Water-bodies also increased from 5,733.49 km² to 5,937.56 km² due to storm surges and water logging accompanied by Amphan. On the other hand, a large decrease was observed for the vegetation due to massive destruction and saltwater intrusion, which converted agriculture and other vegetated areas to salt marshes, thereby increasing barren lands due to the cyclone. In the west and north-east part of the Indian Sundarbans, bareness increased as the super cyclone passed through (Mishra et al., 2021).

4 Conclusion(s)

The research aimed to study the impact of the cyclone Amphan in the Indian Sundarbans using remote sensing multispectral imagery. It can be concluded that the cyclone Amphan caused a devastating impact on the landscape in the Sundarban mangrove ecosystem. NDVI and EVI values revealed massive fragmentation and degradation of mangrove plants, resulting in a shift in land cover from dense to sparse. Barren land extracted from NDBaI index showed that the area of barren land increased by 50.37% after the cyclone. Salinity indices showed a rapid increase, which indicated that the super cyclone resulted in saltwater intrusion. According to the results of the NDWI, the area of water-bodies increased by 160.576 km². More intensive research is needed to estimate and comprehend the ecological damage caused by cyclones, as their frequency and intensity are increasing due to climate change.

Acknowledgement

This research did not receive any specific grant from funding agencies in the public, commercial, or not-for-profit sectors.

Author Contributions

S.P.: Formal analysis, Methodology, Writing -original draft, A.V.: Conceptualization, Supervision, Reviewing and Editing, A.A.S.: Reviewing, and B.K.R: Expert Consultant.

Conflict of Interest

The authors declare no conflict of interest.

References

Akbar Hossain, K., Masiero, M., Pirotti, F., 2022. Land cover change across 45 years in the world's largest mangrove forest (Sundarbans): the contribution of remote sensing in forest monitoring. European Journal of Remote Sensing: 1-17. DOI:https://doi.org/10.1080/22797254.2022.2097450

Akber, M. A., Patwary, M. M., Islam, M. A., Rahman, M. R., 2018. Storm protection service of the Sundarbans mangrove forest, Bangladesh. Natural Hazards, 94: 405-418. DOI:https://doi.org/10.1007/s11069-018-3395-8

Baloloy, A. B., Blanco, A. C., Ana, R. R. C. S., Nadaoka, K., 2020. Development and application of a new mangrove vegetation index (MVI) for rapid and accurate mangrove mapping. ISPRS Journal of Photogrammetry and Remote Sensing, 166: 95-117. DOI:https://doi.org/10.1016/j.isprsjprs.2020.06.001

Chen, X.-L., Zhao, H.-M., Li, P.-X., Yin, Z.-Y., 2006. Remote sensing image-based analysis of the relationship between urban heat island and land use/cover changes. Remote sensing of environment, 104(2): 133-146. DOI:https://doi.org/10.1016/j.rse.2005.11.016

Dutta, D., Das, P. K., Paul, S., Sharma, J. R., Dadhwal, V. K., 2015. Assessment of ecological disturbance in the mangrove forest of Sundarbans caused by cyclones using MODIS time-series data (2001–2011). Natural Hazards, 79: 775-790. DOI:https://doi.org/10.1007/s11069-015-1872-x

Dutta, S., Dutta, I., Das, A., Guchhait, S. K., 2020. Quantification and mapping of fragmented forest landscape in dry deciduous forest of Burdwan Forest Division, West Bengal, India. Trees, Forests and People, 2: 100012. DOI:https://doi.org/10.1016/j.tfp.2020.100012

Elhag, M., Bahrawi, J. A., 2017. Soil salinity mapping and hydrological drought indices assessment in arid environments based on remote sensing techniques. Geoscientific Instrumentation, Methods and Data Systems, 6(1): 149-158. DOI:https://doi.org/10.5194/gi-6-149-2017

Ghosh, A., Schmidt, S., Fickert, T., Nüsser, M., 2015. The Indian Sundarban mangrove forests: history, utilization, conservation strategies and local perception. Diversity, 7(2): 149-169. DOI:https://doi.org/10.3390/d7020149

Giri, C., Pengra, B., Zhu, Z., Singh, A., Tieszen, L. L., 2007. Monitoring mangrove forest dynamics of the Sundarbans in Bangladesh and India using multi-temporal satellite data from 1973 to 2000. Estuarine, coastal and shelf science, 73(1-2): 91-100. DOI:https://doi.org/10.1016/j.ecss.2006.12.019

Hoque, M. A.-A., Phinn, S., Roelfsema, C., Childs, I., 2017. Tropical cyclone disaster management using remote sensing and spatial analysis: A review. International Journal of Disaster Risk Reduction, 22: 345-354. DOI:https://doi.org/10.1016/j.ijdrr.2017.02.008

Hunt Jr, E. R., Rock, B. N., 1989. Detection of changes in leaf water content using near-and middle-infrared reflectances. Remote Sensing of Environment, 30(1): 43-54. DOI:https://doi.org/10.1016/0034-4257(89)90046-1

Jaman, M. H., Rafiq, M. R., Nahin Rezwan, M., Islam, S., Mia, A. J., 2019. NDVI Based Vegetation Change Detection of Sundarbans Due to the Effect of Cyclone 'Bulbul'. Barishal University Journal Part 1, 6(2): 23-35.

Kamble, B., Kilic, A., Hubbard, K., 2013. Estimating crop coefficients using remote sensing-based vegetation index. Remote sensing, 5(4): 1588-1602. DOI:https://doi.org/10.3390/rs5041588

Klemas, V. V., 2009. The Role of Remote Sensing in Predicting and Determining Coastal Storm Impacts. Journal of Coastal Research, 25(6): 1264-1275. DOI:https://doi.org/10.2112/08-1146.1

Krishnamohan, K., Mohanakumar, K., Joseph, P., 2014. Climate change in tropical cyclones and monsoon depressions of North Indian Ocean. In: U. C. Mohanty, M. Mohapatra, O. P. Singh, B. K. Bandyopadhyay, L. S. Rathore, (Ed.), Monitoring and prediction of tropical cyclones in the indian ocean and climate change, pp. 33-39. 10.1007/978-94-007-7720-0_3.

McFeeters, S. K., 1996. The use of the Normalized Difference Water Index (NDWI) in the delineation of open water features. International journal of remote sensing, 17(7): 1425-1432. DOI:https://doi.org/10.1080/01431169608948714

Mishra, A. K., Vanganuru, N., 2020. Monitoring a tropical super cyclone Amphan over Bay of Bengal and nearby region in May 2020. Remote Sensing Applications: Society and Environment, 20: 100408. DOI:https://doi.org/10.1016/j.rsase.2020.100408

Mishra, M., Acharyya, T., Santos, C. A. G., da Silva, R. M., Kar, D., Kamal, A. H. M., Raulo, S., 2021. Geo-ecological impact assessment of severe cyclonic storm Amphan on Sundarban mangrove forest using geospatial technology. Estuarine, Coastal and Shelf Science, 260: 107486. DOI:https://doi.org/10.1016/j.ecss.2021.107486

Mondal, M., Haldar, S., Biswas, A., Mandal, S., Bhattacharya, S., Paul, S., 2021. Modeling cyclone-induced multi-hazard risk assessment using analytical hierarchical processing and GIS for coastal West Bengal, India. Regional Studies in Marine Science, 44: 101779. DOI:https://doi.org/10.1016/j.rsma.2021.101779

Moreira, L. C. J., Teixeira, A. d. S., Galvão, L. S., 2015. Potential of multispectral and hyperspectral data to detect saline-exposed soils in Brazil. GIScience & Remote Sensing, 52(4): 416-436. DOI:https://doi.org/10.1080/15481603.2015.1040227

Paul, B. K., 2009. Why relatively fewer people died? The case of Bangladesh's Cyclone Sidr. Natural Hazards, 50: 289-304. DOI:https://doi.org/10.1007/s11069-008-9340-5

Rasul, A., Balzter, H., Ibrahim, G. R. F., Hameed, H. M., Wheeler, J., Adamu, B., Ibrahim, S. a., Najmaddin, P. M., 2018. Applying Built-up and Bare-soil Indices from Landsat 8 to Cities in Dry Climates. Land, 7(3): 81. DOI:https://doi.org/10.3390/land7030081

Rouse, J. W., Haas, R. H., Schell, J. A., Deering, D. W., 1973. Monitoring vegetation systems in the greant plains with ERTS: . Proceedings of the Earth Resources Technology Satellite Symposium NASA SP-351, Vol. 1, Washington, DC: NASA, pp. 309–317.

Sakib, M., 2015. Sundarban as a Buffer Against Storm Surge Flooding. World Journal of Engineering and Technology, 3(03): 59. DOI:10.4236/wjet.2015.33C009